Research Article

In Vitro-Based Prediction of Human Plasma Concentrations of Food-Related Compounds

Takashi Kitaguchi[1], Mina Ito[1], Katsutoshi Ohno[1], Noriaki Ota[1], Kazuhiro Kobayashi[1], Hiromi Sato[2], Takahiro Iwao[3], Tamihide Matsunaga[3], Mitsuru Tanaka[1] and Akihiro Hisaka[2]

[1]Global Food Safety Institute, Nissin Foods Holdings Co., Ltd, Hachioji, Tokyo, Japan; [2]Laboratory of Clinical Pharmacology and Pharmacometrics, Graduate School of Pharmaceutical Sciences, Chiba University, Chiba, Chiba, Japan; [3]Department of Clinical Pharmacy, Graduate School of Pharmaceutical Sciences, Nagoya City University, Nagoya, Aichi, Japan

Abstract

Efforts have been made to replace animal experiments in safety evaluations, including *in vitro*-based predictions of human internal exposures, such as predicting peak plasma concentration (C_{max}) values for xenobiotics and comparing these values with *in vitro*-based toxicity endpoints. Herein, the authors predicted the C_{max} values of food-related compounds in humans based on existing and novel *in vitro* techniques. In this study, 20 food-related compounds, which have been previously reported in human pharmacokinetic or toxicokinetic studies, were evaluated. Human induced pluripotent stem cell-derived small intestinal epithelial cells (hiPSC-SIEC) and Caco-2 cells, HepaRG cells, equilibrium dialysis of human plasma, and LLC-PK1 cell monolayer were used to assess intestinal absorption and availability, hepatic metabolism, unbound plasma fraction, and secretion and reabsorption in renal tubular cells, respectively. After conversion of these parameters into human kinetic parameters, the plasma concentration profiles of these compounds were predicted using *in silico* methods, and the obtained C_{max} values were found to be between 0.017 and 183 times the reported C_{max} values. When the *in silico*-predicted parameters were modified with *in vitro* data, the predicted C_{max} values came within 0.1-10 times the reported values because the metabolic activities of hiPSC-SIECs, such as uridine 5′-diphospho-glucuronosyl transferase, are more similar to those of human primary enterocytes. Thus, combining *in vitro* test results with the plasma concentration simulations resulted in more accurate and transparent predictions of C_{max} values of food-related compounds than those obtained using *in silico*-derived predictions alone. This method facilitates accurate safety evaluation without the need for animal experiments.

1 Introduction

Conventional risk assessment methods rely on animal testing. Alternative testing methods focus on hazard identification and characterization without the use of animals (EFSA, 2014; Gocht et al., 2015; Kojima, 2019). A new paradigm called next generation risk assessment (NGRA) was proposed for quantitative risk assessment without animal testing. NGRA is defined as an exposure-led, hypothesis-driven risk assessment approach that integrates new approach methodologies (NAMs), i.e., *in silico*, *in chemico*, and *in vitro* methodologies (Dent et al., 2018). Using NGRA, human physiological conditions can be reproduced more closely by using human physiologically based kinetic (PBK) models rather than relying on conventional *in vitro*-based toxicity assays alone, as shown in several case studies (Baltazar et al., 2020; Vandecasteele et al., 2021; Bury et al., 2021; Terasaka et al., 2022). Especially, for orally ingested chemicals, these efforts include *in silico* and/or *in vitro*-based predictions of human internal exposures, such as C_{max} values for xenobiotics (Punt et al., 2022; Terasaka et al., 2022; Kamiya et al., 2022).

Food consists of a mixture of several compounds, including chemicals added or produced during processing and storage stages. Limited information about the pharmacokinetics, i.e., the absorption, distribution, metabolism, and elimination (ADME), of certain compounds raises concerns about assessing their risk to human health. It has been suggested that NGRA approaches should be transferable from cosmetics to food-related compounds (Ohta et al., 2022).

Although *in silico* prediction is especially useful for initial risk assessment screening, its prediction accuracy is highly depen-

Received February 13, 2023; Accepted May 10, 2023;
Epub May 12, 2023;

ALTEX 40(4), 595-605. doi:10.14573/altex.2302131

Correspondence: Takashi Kitaguchi, PhD
Global Food Safety Institute, Nissin Foods Holdings Co., Ltd.
2100 Tobuki-machi, Hachioji, Tokyo, 192-0001, Japan
(takashi.kitaguchi@nissin.com)

dent on the data sets used to create the prediction models. These prediction models are often built on data from pharmaceuticals due to the availability of detailed pharmacokinetic measurements in humans. As pharmacokinetic measurements regarding certain food-related chemicals is scarce, the direct applicability of these models to predicting the pharmacokinetics of food-related compounds is limited. An *in vitro*-based approach is required to overcome the above-mentioned issues as such an approach includes mechanistic information obtained using cellular and/or tissue-mimicking assay systems.

Previously, the authors have demonstrated the membrane permeability of food-related compounds using uridine 5'-diphospho-glucuronosyl transferase (UGT)-mediated intestinal metabolism in human-induced pluripotent stem cell-derived small intestinal cells (hiPSC-SIECs). These cells are more predictive of human physiology than Caco-2 cells (derived from cultured human colon cancer cells), which are considered the gold standard (Kitaguchi et al., 2021).

This study mimicked typical human ADME processes using existing and novel *in vitro* techniques, converted the *in vitro* data into human PBK parameters, and performed simulations using a human PBK model to evaluate the pharmacokinetic parameters of food-related compounds. Finally, the prediction accuracy of the C_{max} values of 20 food-related test compounds was demonstrated by comparison with corresponding plasma concentrations in humans.

2 Materials and methods

2.1 Cells and reagents

hiPSC-SIECs were purchased from Fujifilm Wako (F-hiSIEC™, Osaka, Japan), which included seeding and maintenance medium. Preplated human colon carcinoma Caco-2 cells (passage numbers 55-65) were purchased from ReadyCell (CacoReady™ Plate, Barcelona, Spain). The human hepatoma cell line HepaRG® was purchased from KAC (Kyoto, Japan). LLC-PK1 porcine kidney proximal tubular cells at passage 196 (ATCC CL-101™) were obtained from the American Type Culture Collection (ATCC, Manassas, VA). Dulbecco's modified Eagle's medium (DMEM), penicillin-streptomycin solution, non-essential amino acids solution (NEAA), and fetal bovine serum (FBS) were purchased from Thermo Fisher Scientific (Waltham, MA, USA). Hanks' balanced salt solution (HBSS) and dimethyl sulfoxide (DMSO) were procured from Fujifilm Wako.

All drugs, food-related compounds, and metabolites listed below were dissolved in DMSO and stored at -20°C until further use. Curcumin, bisphenol A, 2-amino-3,8-dimethylimidazo[4,5-f] quinoxaline (MeIQx), and 7-hydroxycoumarin were procured from Fujifilm Wako. Acrylamide, fenitrothion, and β-estradiol were purchased from Sigma-Aldrich (St. Louis, MO, USA). Bisphenol S, picloram, and raloxifene were purchased from Tokyo Chemical Industry (Tokyo, Japan). Daidzein and genistein were purchased from LC Laboratories (Woburn, MA, USA). Quercetin, diclofenac, telmisartan, and troglitazone were purchased from Nacalai Tesque (Kyoto, Japan).

2.2 Membrane permeability assay using hiPSC-SIECs and Caco-2 cells

hiPSC-SIECs were thawed and seeded at an initial density of 1×10^5 cells/well in Matrigel-coated 24-well cell culture inserts (Merck Millipore, Burlington, MA, USA) and then maintained for 9-13 days according to the manufacturer's instruction. Preplated Caco-2 cells were shipped on day 18 after seeding into 24-well cell culture inserts and maintained with DMEM supplemented with 1% NEAA, 10% FBS, and 50 U/mL penicillin/streptomycin for an additional 3-7 days according to the suppliers' instructions. Transepithelial electronic resistance (TEER) values were measured with Millicell ERS-2 (Merck Millipore) immediately before and after the membrane permeability assays to ensure maintenance of the membrane barrier during the assays.

The assays were conducted according to a previously described method (Kitaguchi et al., 2021). Briefly, hiPSC-SIECs (n = 2) and Caco-2 cells (n = 3) were washed thrice with apical and basal transport buffers (HBSS containing 10 mM MES and 4.5 g/L glucose at pH 6.5 and 7.4, respectively) in chambers and incubated at 37°C for at least 30 min. Membrane transport assays were performed at 37°C for 30, 60, and 90 min after replenishing the apical chambers with transport buffer containing each substrate at a final concentration of 10 μM. The solution was collected from the basal chambers at 30 min intervals, diluted with an equal volume of acetonitrile, and stored at -20°C. Unreacted substrates were measured using ultraperformance liquid chromatography-tandem mass spectrometry (UPLC-MS/MS).

The apparent permeability coefficients (P_{app}) were calculated using the following equation:

$$P_{app} = dQ/dt \times [1/(A \times C_0)] \quad \text{Eq. 1}$$

where dQ/dt, A, and C_0 represent the amount of permeated compound per unit of time, the surface area of the transport membrane, and the initial compound concentration in the donor chamber, respectively.

2.3 Plasma protein binding assays for predicting the volume of distribution

The unbound fraction in human plasma (f_{up}) was determined by the equilibrium dialysis method with a Rapid Equilibrium Dialy-

Abbreviations
ADME, absorption, distribution, metabolism, and elimination; C_{max}, peak plasma concentration; CYP, cytochrome P450; DMEM, Dulbecco's modified Eagle's medium; DMSO, dimethyl sulfoxide; F_a, fraction absorbed from the intestine; F_g, fraction escaping intestinal metabolism; F_h, fraction escaping hepatic metabolism; FBS, fetal bovine serum; HBSS, Hanks' balanced salt solution; hiPSC-SIEC, human induced pluripotent stem cell-derived small intestinal epithelial cell; MeIQx, 2-amino-3,8-dimethylimidazo[4,5-f]quinoxaline; MES, 2-(N-morpholino)ethanesulfonic acid; NAMs, new approach methodologies; NEAA, nonessential amino acids solution; NGRA, next generation risk assessment; P_{app}, apparent permeability coefficient; PBK, physiologically based kinetic; UGT, uridine 5'-diphospho-glucuronosyl-glucuronosyltransferase; UPLC-MS/MS, ultraperformance liquid chromatography-tandem mass spectrometry

sis device (Thermo Fisher Scientific) according to the manufacturer's instructions. Briefly, human plasma (Takara Bio) was dialyzed against phosphate buffer (pH 7.2) using a membrane with a nominal cutoff of 8 kDa at 37°C for 4 h with gentle agitation (n = 3). The final concentration of each compound added to the plasma was 2 or 20 µM depending on the detection sensitivity of UPLC-MS/MS. Equal volumes of either buffer (to the plasma samples) or compound-free plasma (to the buffer samples) were added, followed by protein precipitation with acetonitrile (performed four times) and filtration with FastRemover (GL Science, Tokyo, Japan) for UPLC-MS/MS.

The f_{up} of each compound was calculated as the concentration of the buffer sample divided by the concentration of the plasma sample.

2.4 Metabolic stability assay using HepaRG cells for predicting hepatic clearance

HepaRG cell culture and metabolic stability assays were performed as described previously (Bonn et al., 2016). Briefly, the cryopreserved HepaRG cells were thawed and 100 µL cell suspension (0.72×10^6 cells/mL) was seeded into each well of flat-bottomed 96-well plates coated with type 1 collagen. They were allowed to attach for approximately 24 h in a CO_2 incubator, and the medium was renewed with HepaRG culture medium at room temperature. After 60 h, the medium was renewed with HepaRG serum-free induction medium, and 24 h later, the cells were exposed to the compounds for 0.25, 0.5, 1, 2, 4, 8, and 24 h (n = 3). After the incubation, the supernatants from each well were collected and diluted three times with ice-cold acetonitrile containing 0.8% formic acid. The samples were centrifuged at 4°C for 10 min at 10,000 g, and aliquots of the clear supernatant were diluted with equal amounts of water and kept at 4°C until UPLC-MS/MS analysis.

In vitro intrinsic hepatic clearance ($CL_{h,int}$) was calculated from the parent compound loss data according to Bonn et al. (2016) using the following equation:

$$CL_{h,int} = -slope\ of\ ln\ (\%\ drug\ remaining)\ vs\ time\ plot \times mL\ incubation\ /\ 10^6\ cells\ (\mu L \cdot min^{-1} \cdot 10^6\ cells^{-1}) \quad \text{Eq. 2}$$

2.5 Bidirectional membrane permeability assay using LLC-PK1 cells for predicting urinary clearance

These assays were conducted as described by Kunze et al. (2014) with minor modifications. LLC-PK1 cells were cultured in medium 199 (Thermo Fisher Scientific) supplemented with 10% FBS at 37°C in a 5% CO_2 incubator. The medium was changed every second to third day. The cells were cultivated for a maximum of 2 months and were passaged 16 times.

Bidirectional transport assays were conducted in 24-well cell culture inserts (Corning, Corning, NY). The LLC-PK1 cells were seeded into 24-well cell culture inserts with a microporous polyethylene terephthalate membrane (0.4 µm pore size; 0.33 cm^2 surface area) at a density of 4×10^4 cells/cm^2. The cells were maintained for four days as described above. The experiments were performed in modified Krebs buffer adjusted to pH 7.4 for the basolateral (1 mL) and 6.8 for the apical (0.2 mL) compartments. The cells on the inserts were washed thrice with prewarmed assay buffer, and then preincubated with buffer in both compartments for at least 30 min. Subsequently, the buffer from the apical chamber was aspirated and replaced with buffer containing test compound (1 µM). After incubation for 30 and 60 min at 37°C (n = 3), aliquots (0.1 mL) from both compartments were sampled and quantified with UPLC-MS/MS.

The P_{app} values in basolateral to apical ($P_{app,BA}$) and apical to basolateral ($P_{app,AB}$) directions were determined using Eq. 1. The $P_{app,BA}$ and $P_{app,AB}$ values were upscaled to human intrinsic renal clearances ($CL_{r,int,BA}$ and $CL_{r,int,AB}$) using the following equation:

$$CL_{r,int} = P_{app} \times \pi \times l_{PT} \times d_{PT} \times n_{neph} \times n_{kid} / BW \quad \text{Eq. 3}$$

where the surface of a human proximal tubule is calculated as the product of its length l_{PT} (1.5 cm), its diameter d_{pt} (7×10^{-3} cm), and the number pi ($\pi = 3.14$). n_{neph} is the number of nephrons per kidney (1.5×10^6), n_{kid} the number of kidneys per human (2), and BW is the average human body weight (70 kg).

2.6 Data conversion from *in vitro* data to human PBK parameters

Determination of absorptive constant (k_a)

The experimental P_{app} values of Caco-2 cells were converted to the effective permeability coefficient (P_{eff}) using GastroPlus (ver. 9.8.2., Simulations Plus, Lancaster, CA) P_{eff} converter with human P_{eff} reported compounds. k_a (10^{-3} min^{-1}) was derived from P_{eff} according to the previous literature (Sugano, 2012) with the following equation:

$$k_a = 2 \times DF / R_{GI} \times P_{eff} \quad \text{Eq. 4}$$

where DF is the degree of flatness of the gastrointestinal tract (1.7), and R_{GI} is the radius of the gastrointestinal tract (1.5 cm).

Determination of fraction escaping intestinal metabolism (F_g)

F_g was estimated using a previously described method (Michiba et al., 2022) using the following equation:

$$F_g = 1 / [(2 \times CL_{AtoB,+inh} / CL_{AtoB,-inh}) - 1] \quad \text{Eq. 5}$$

where $CL_{AtoB,+inh}$ and $CL_{AtoB,-inh}$ represent the apical-to-basolateral transcellular transport clearance in the absence and presence of a metabolic inhibitor, respectively.

In this study, Caco-2 cells were assumed to possess negligible metabolic activity (Kitaguchi et al., 2021), whereas other factors such as transporter- and paracellular-mediated permeation were assumed to be similar in Caco-2 cells and hiPSC-SIECs. These assumptions suggested that the relationship of $CL_{AtoB,+inh}$ / $CL_{AtoB,-inh}$ ratio and P_{app} of Caco-2 cells/P_{app} of hiPSC-SIECs ratio are equal, and these values were substituted in the above equation.

Determination of hepatic clearance (CL_h) and fraction escaping hepatic metabolism (F_h)
CL_h (mL/min/kg) was estimated based on a previous study (Bonn et al., 2016) using the following equation:

$$CL_h = CL_{h,int} \times 120 \times 10^6\ cells/g\ liver \times 24\ g\ liver/BW \times f_{u,b} / f_{u,inc} \quad \text{Eq. 6}$$

where $f_{u,b}$ is a fraction of unbound compound in the blood and was calculated as per a previous report (Hallifax et al., 2010), and $f_{u,inc}$ is a fraction of unbound compound after *in vitro* incubation predicted from a previous report (Kilford et al., 2008).

The F_h was calculated from CL_h and $f_{u,b}$ using the following equation according to a well-stirred model.

$$F_h = Q_h / (Q_h + f_{u,b} \times CL_h) \quad \text{Eq. 7}$$

Q_h represents the hepatic blood flow rate [20.7 mL/(min · kg)].

Determination of renal clearance (CL_r)
The CL_r (mL/min/kg) is a composed process involving glomerular filtration clearance ($CL_{r,fil}$), tubular secretion clearance ($CL_{r,sec}$), metabolic clearance, and reabsorption of a fraction of the drug from the tubule fluid back into the blood (f_{reab}). Assuming that the contribution of renal metabolic clearance is negligible, $CL_{r,org}$ can be expressed using the following equations (Kunze et al., 2014):

$$CL_r = (CL_{r,fil} + CL_{r,sec}) \cdot (1 - f_{reab})$$
$$CL_{r,fil} = f_{u,b} \cdot GFR$$
$$CL_{r,sec} = Q_{r,b} \cdot f_{u,b} \cdot CL_{r,int,BA} / (Q_{r,b} + f_{u,b} \cdot CL_{r,int,BA})$$
$$f_{reab} = CL_{r,int,AB} / (GFR + CL_{r,int,AB}) \quad \text{Eq. 8}$$

where GFR is the glomerular filtration rate [1.79 mL/(min · kg)] and $Q_{r,b}$ is the renal blood flow rate [17.14 mL/(min · kg)].

Determination of the volume of distribution (V_d)
The V_d (L) was calculated according to previous reports (Øie and Tozer, 1979; Waters and Lombardo, 2010) using the following equation:

$$V_d = V_P (1 + R_{E/I}) + f_{up} \cdot V_P (V_E / V_P - R_{E/I}) + V_R \cdot f_{up} / f_{ut} \quad \text{Eq. 9}$$

where f_{ut} is the fraction unbound in tissues and $R_{E/I}$ is the extravascular: intravascular ratio of binding proteins (usually 1.4 for albumin). V_P, V_E, and V_R refers to the volumes of plasma, extracellular fluid, and remainder fluid with values of 0.0436, 0.151, and 0.38 L/kg, respectively, in humans.

f_{ut} was predicted according to a previous study (Berellini and Lombardo, 2019) using the following equation:

$$Log\ f_{ut} = -0.249 \cdot log\ D_{7.4} - 0.999 \cdot f_{i,7.4} + 0.735 \cdot \log f_{up} + 0.070 \quad \text{Eq. 10}$$

where $f_{i,7.4}$ is the cationic fraction ionized at pH 7.4.

Determination of elimination constant (k_e)
The k_e (10^{-3} min^{-1}) was calculated using the following equation:

$$k_e = (CL_h + CL_r) / V_d \quad \text{Eq. 11}$$

Prediction of in silico *physicochemical and human kinetic parameters*
All physicochemical and kinetic parameters (pKa, LogP, k_a, first pass, k_e, and V_d) were directly predicted using ACD/Percepta (2017.2). Prediction of LogP and pKa are from QSAR (quantitative structure activity relationships) model on the basis of GALAS (global, adjusted locally according to similarity) modeling methodology (Sazonovas et al., 2010). Prediction of k_a and V_d are from previously reported QSAR models (Reynolds et al., 2009; Lanevskij et al., 2010), and k_e and first pass are from the empirical model based on fragment structure descriptors and partial least squares regression statistics (personal communication).

2.7 Prediction of human plasma concentrations using simulation software

The PK Explorer module in ACD/Percepta (2017.2) was used to predict human plasma concentration profiles. The module consisted of differential equations involving solubility in the gastrointestinal tract, k_a, first-pass metabolism in the gut and liver ($1 - F_g \times F_h$), V_d, and k_e. The solubility in the gastrointestinal tract was predicted from aqueous solubility corrected for the solubilizing effect of bile salts, and the other parameters were replaced with the *in silico*-predicted values described above. The predictions of human plasma concentrations were based on the compartmental absorption and transit model as previously reported (Yu and Amidon, 1999) (personal communication).

3 Results

3.1 Assessment of absorption and F_g using Caco-2 cells and hiPSC-SIECs

Figure 1 shows the P_{app} values obtained using Caco-2 cells and hiPSC-SIECs of 20 food-related compounds. The P_{app} values in hiPSC-SIECs were 3.1-53 times lower than those in Caco-2 cells for quercetin, curcumin, daidzein, daidzin, genistein, genistin, bisphenol A, bisphenol S, and ferulic acid, which are known UGT-metabolized compounds. However, the P_{app} values of cyanidin 3-glucoside and caffeic acid in hiPSC-SIECs were 5.6-7.7 times higher than those in Caco-2 cells. Furthermore, P_{app} values were determined using Caco-2 cells and hiPSC-SIECs for the reported UGT-metabolized drugs in the small intestine, including raloxifene, diclofenac, telmisartan, and troglitazone. As shown in Table 1, the P_{app} values for these drugs were 1.2-15 times lower in hiPSC-SIECs than in Caco-2 cells.

The F_g values of these drugs were calculated using the conversion formula (Michiba et al., 2022). As shown in Table 1, the calculated F_g values of the four drugs with reported F_a (fraction absorbed from the intestine) × F_g or F_g values were comparable to the previously reported $F_a \times F_g$ or F_g in humans (Nakamori et al.,

Tab. 1: P_{app} values using Caco-2 cells and hiPSC-SIECs, and calculated F_g or $F_a \times F_g$ of reported drugs and food-related compounds

Compound	P_{app} ($\times 10^{-6}$ cm/s)		F_g or $F_a \times F_g$		
	Caco-2 cells	hiPSC-SIECs	Calculated F_g	Reported F_g	Reported $F_a \times F_g$
Quercetin	9.89 ± 0.636	0.463	0.025	–	0.003[a], 0.0165[c]
Curcumin	3.50 ± 0.805	0.0666	0.0096	–	–
Daidzein	36.8 ± 1.55	1.59	0.022	–	–
Daidzin*	0.0574 ± 0.00854	0.0150	0.150	–	–
Genistein	33.7 ± 1.02	2.68	0.041	–	0.0375[c]
Genistin*	0.0910 ± 0.0275	0.00925	0.054	–	–
Bisphenol A	29.7 ± 2.23	4.29	0.078	–	–
Bisphenol S	23.4 ± 0.742	5.85	0.143	–	–
Ferulic acid	24.6 ± 2.03	7.86	0.190	–	–
Raloxifene	2.44 ± 0.327	0.164	0.035	–	0.069[a]
Diclofenac	47.5 ± 1.43	35.3	0.591	0.685[b]	0.738[a]
Telmisartan	35.3 ± 0.707	30.4	0.758	0.674[b]	1.00[a]
Troglitazone	7.34 ± 0.308	4.80	0.486	0.558[b]	–

Each P_{app} data represents the mean ± S.D. of n = 3 (Caco-2 cells) or means of n = 2 (hiPSC-SIECs). [a] Nakamori et al., 2012. The values are calculated using the hepatic blood flow rate of 20.7 mL/min/kg. [b] Nishimuta et al., 2011. [c] Kikuchi et al., 2022. The values are from the allometric scaling-based-$F_a \times F_g$ calculation method.

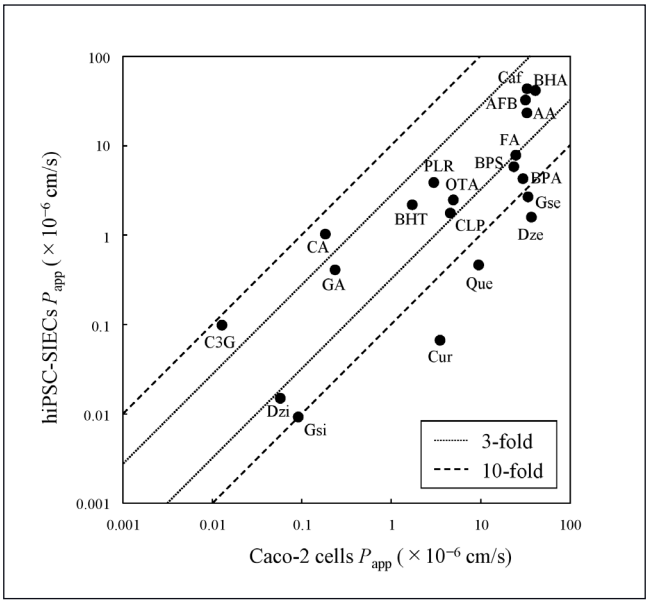

Fig. 1: Comparison between the P_{app} values of Caco-2 cells and hiPSC-SIECs obtained using membrane permeability assays

The P_{app} values obtained from Caco-2 cells and hiPSC-SIECs were plotted. The dotted and dashed lines represent the P_{app} values of Caco-2 cells and hiPSC-SIECs that were within 3-fold and 10-fold, respectively. The compounds used are as follows: Dzi, daidzin*; Dze, daidzein; Gsi, genistin*; Gse, genistein; Que, quercetin; GA, gallic acid; CA, caffeic acid; FA, ferulic acid; C3G, cyanidin 3-glucoside; Cur, curcumin; Caf, caffeine; AA, acrylamide; BHA, butylated hydroxyanisole; BHT, butylated hydroxytoluene; AFB, aflatoxin B1; OTA, ochratoxin A; BPA, bisphenol A; BPS, bisphenol S; CLP, chlorpyrifos; PLR, picloram. These compounds were tested at a concentration of 10 μM. Each plot represents the mean of n = 3 (Caco-2 cells) or n = 2 (hiPSC-SIECs). The *P_{app} values of daidzin and genistin were detected as daidzein and genistein.

2012; Nishimuta et al., 2011; Kikuchi et al., 2022). Therefore, the F_g conversion formula was also applied to the test compounds, which exhibited higher P_{app} values in Caco-2 cells than in hiPSC-SIECs (Tab. 1). The F_g ranged from 0.0096 to 0.19. Moreover, the calculated F_g values of quercetin (0.025) and genistein (0.041) were comparable to their reported $F_a \times F_g$ values (quercetin: 0.003 and 0.0165; genistein: 0.0375, respectively).

3.2 Comparison between the *in silico*-predicted and *in vitro*-derived values for human PBK parameters

The *in vitro*-derived parameters were converted to human PBK parameters (k_a, first-pass metabolism in the gut and liver, k_e, and V_d) with a previously reported conversion formula described in the Materials and Methods section. The obtained values were then compared with the *in silico*-predicted values (Fig. 2A-D).

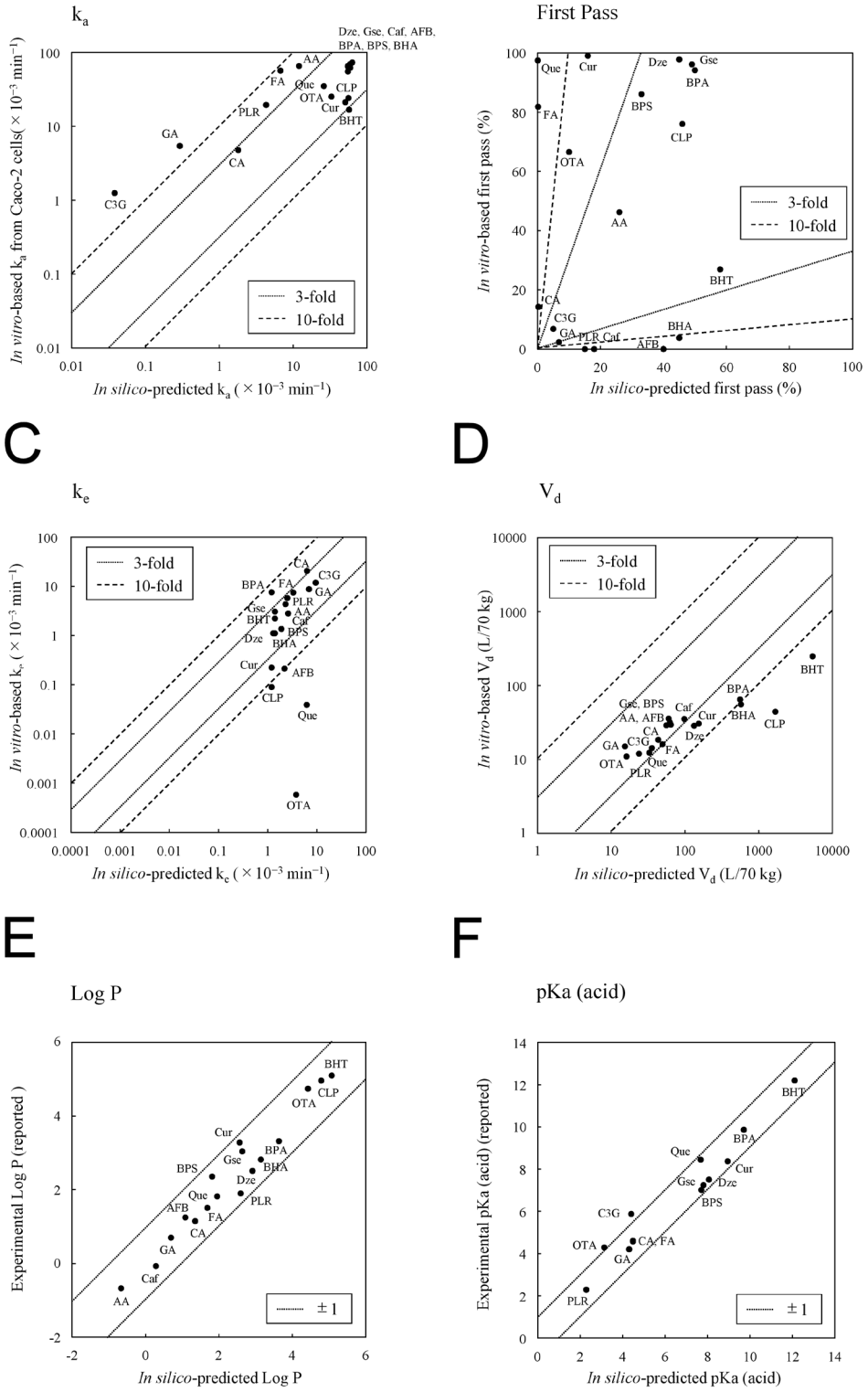

Fig. 2: The comparison between *in silico*-predicted and *in vitro*-derived or reported values for evaluating kinetic and physicochemical parameters

The *in silico*-predicted and *in vitro*-derived values of the test compounds were plotted for the following parameters: A) absorption rate constant (k_a) from Caco-2 cells, B) first pass, C) elimination rate constant (k_e), and D) volume of distribution (V_d); the dotted and dashed lines represent the values that are within 3-fold and 10-fold, respectively. The *in silico*-predicted and reported values were plotted against E) partition coefficient (Log P) and F) acidity constant (pKa); the dotted lines represent the values that are between −1 and 1. The compounds plotted are as follows: Dze, daidzein; Gse, genistein; Que, quercetin; GA, gallic acid; CA, caffeic acid; FA, ferulic acid; C3G, cyanidin 3-glucoside; Cur, curcumin; Caf, caffeine; AA, acrylamide; BHA, butylated hydroxyanisole; BHT, butylated hydroxytoluene; AFB, aflatoxin B1; OTA, ochratoxin A; BPA, bisphenol A; BPS, bisphenol S; CLP, chlorpyrifos; PLR, picloram.

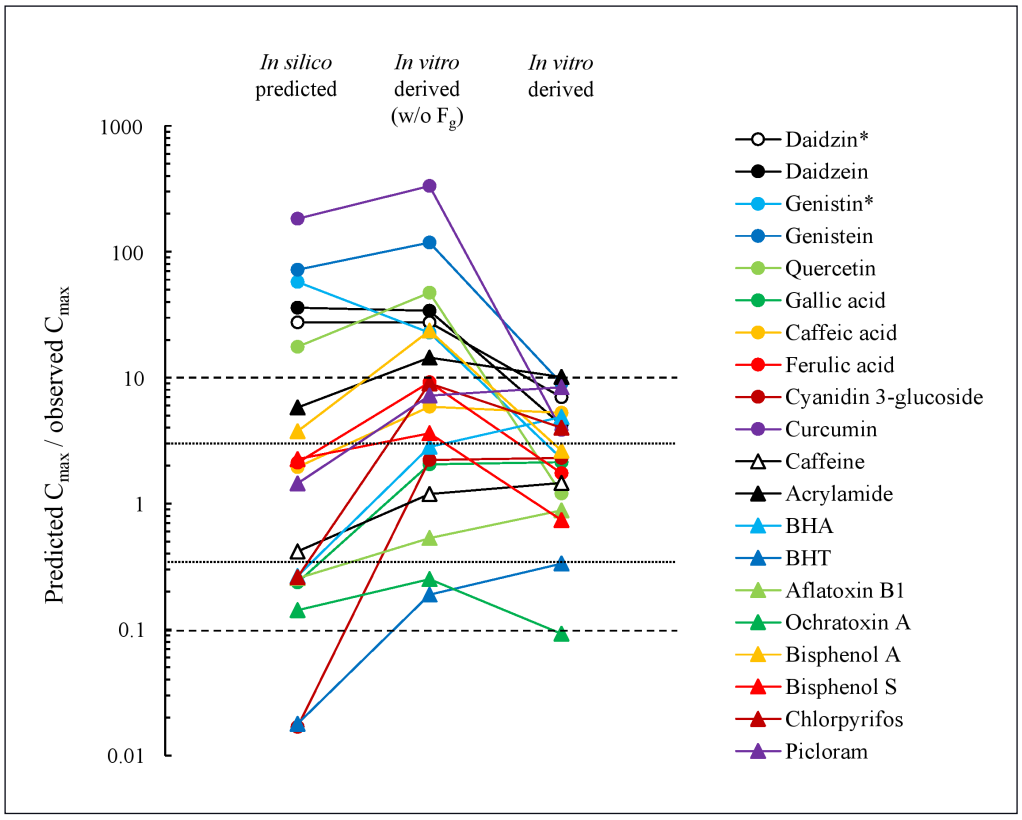

Fig. 3: Comparison between the predicted and observed C_{max} values from 20 food-related compounds
The *in silico* predicted C_{max} values, *in vitro*-based C_{max} values with *in silico* predicted first pass, and *in vitro*-based C_{max} values divided by the reported human C_{max} values from previous literature were plotted. The dotted and dashed lines represent the predicted values that are within 3-fold and 10-fold, respectively. *C_{max} values of daidzin and genistin were predicted as daidzein and genistein.

Moreover, the predicted values for the physicochemical parameters, Log P and pKa, were compared with those available in the literature (Fig. 2E,F). The details of these values are provided in Table S1 and S2[1].

Regarding k_a, the *in vitro*-derived values tended to be higher than those predicted *in silico* (Fig. 2A). Especially, the *in vitro*-derived k_a of cyanidin 3-glucoside, gallic acid, ferulic acid, picloram, and acrylamide, which have high polarity or low molecular weight characteristics, were more than three-fold higher than the *in silico*-derived values (0.038 vs. 1.2, 0.29 vs. 5.4, 6.7 vs. 56, 4.3 vs. 19, and 12 vs. 65 × 10^{-3} min^{-1}, respectively).

For the first pass and k_e, no apparent relationships were observed between the *in silico*-predicted and *in vitro*-derived values (Fig. 2B,C). In particular, the k_e of ochratoxin A, quercetin, and chlorpyrifos varied considerably, possibly due to the significantly higher plasma protein binding rate (> 99.9%) than the *in silico*-predicted values (Tab. S1[1]).

The *in vitro*-derived V_d values were lower than the *in silico*-predicted values (Fig. 2D). Especially, the *in vitro*-derived V_d for BHT, BHA, and chlorpyrifos were more than 10-fold lower than the *in silico*-derived values (248 vs. 5390, 56 vs. 574, and 43 vs. 1680 L/70 kg, respectively). Moreover, the physicochemical parameters (Log P and pKa) were consistent with the *in silico*-predicted values (Fig. 2E,F).

3.3 Comparison between *in silico*-predicted and *in vitro*-derived values for C_{max}

Figure 3 shows the results of human pharmacokinetic prediction using the PBK parameters obtained above. Detailed data is provided in Table S3[1]. When the plasma concentrations of the food-related test compounds were predicted using only *in silico*-predicted parameters, the C_{max} values of these 20 compounds were between 0.017 and 183 times those of the reported C_{max} values. When the *in silico*-predicted parameters were replaced with the *in vitro* data obtained in this study and reported physicochemical parameters, the predictivity of C_{max} values did not improve (ranging from 0.19 to 333 times the reported C_{max} values). Better predictivity was obtained using the F_g values from hiPSC-SIECs: the predicted C_{max} values of the 20 test compounds were almost within a factor of 10 of the reported C_{max} values (0.092-10.1).

4 Discussion

Prediction of human pharmacokinetics is a key factor for NGRA. Recently, the application of safety evaluation methods without conducting animal experiments has been in high demand, not only for excipients of cosmetics but also for gen-

[1] doi:10.14573/altex.2302131s

eral chemicals, including food-related compounds. Since food-related compounds are orally ingested, predicting their gastrointestinal absorption is essential for predicting human pharmacokinetics. However, reports on the pharmacokinetics of food-related compounds and pharmacokinetics-based predictivity studies without animal testing in humans are limited. This study evaluated the predictivity of C_{max} values using recently reported alternative testing methods and compared it with human pharmacokinetic data of food-related compounds from existing literature.

Caco-2 cells have microvilli-like structures and can be used to predict the oral absorption of compounds that undergo transcellular permeation by passive diffusion (Lea, 2015). Owing to this property, Caco-2 cell monolayers have been used to predict gastrointestinal absorption. These cells also express intestinal efflux transporters such as P-glycoprotein, multidrug resistant protein 2, and breast cancer resistant protein (Lu et al., 2022). However, Caco-2 cells are colon cancer-derived cells and have characteristics that are different from the human small intestine such as an extremely high TEER value and limited expression of metabolic enzymes, including CYP3A and small intestine-specific UGT isoforms (Kabeya et al., 2020; Kitaguchi et al., 2021). In line with this, Punt et al. (2022) reported the predictivity of human plasma C_{max} values of 44 pharmaceuticals and food-related compounds with certain overestimation. They discussed the reasons behind the overestimation compared to existing ADME information and identified several compounds that undergo intestinal metabolism. The prediction of F_g was assumed to be a key factor.

Recently, new cells were developed, and human-derived samples were used for F_g prediction (Michiba et al., 2022). The authors reported significant differences in the membrane permeation rates for a group of compounds undergoing glucuronidation in Caco-2 cells and hiPSC-SIECs. The expression and metabolic activities of UGT isoforms in hiPSC-SIECs were similar or higher than those in human small intestinal cells (Kitaguchi et al., 2021). As several test compounds used in this study are known glucuronidated substrates, an attempt was made to apply the first-pass metabolism in the gut by comparing the permeability data of Caco-2 cells and hiPSC-SIECs. The P_{app} values of hiPSC-SIECs were 3.1-53-fold lower than those in Caco-2 cells. Previously, the authors of this study had reported that the relationships between P_{app} values and F_a or $F_a \times F_g$ of hiPSC-SIECs correlated better than those in Caco-2 cells. However, regression equation-based $F_a \times F_g$ calculation did not correlate well with the reported $F_a \times F_g$ or F_g (data not shown). Therefore, the conversion formula put forth by Michiba et al. (2022) was used to calculate F_g. They calculated CYP3A-derived F_g based on the difference in the permeability of human intestinal organoid-derived cells with and without CYP3A4 inhibitor. It was assumed that Caco-2 cells have negligible UGT metabolic activity and that other factors are similar in Caco-2 cells and hiPSC-SIECs. Based on these assumptions, F_g was calculated, which was found to be comparable to the reported F_g of drugs in humans.

Recently, Kikuchi et al. (2022) reported an allometry-based calculation of human $F_a \times F_g$ values for food-related compounds using existing pharmacokinetic data in rats. This study calculated the $F_a \times F_g$ values for quercetin and genistein, which were 0.0165 and 0.0375, respectively, comparable to predicted F_g values (0.025 and 0.041, respectively). The possible limitation of this calculation method is the assumption that characteristics other than UGT metabolism (e.g., transporter expressions and functions, transcellular permeability, and paracellular permeability) are similar between Caco-2 cells and hiPSC-SIECs. However, the authors did not confirm these characteristics. For example, TEER, which indicates the tightness of the cell-to-cell connection, is significantly different between Caco-2 cells and hiPSC-SIECs. However, the authors reported that the $F_a \times F_g$ and P_{app} slopes of the 20 known drugs are almost the same, regardless of the difference between the TEER values. Both cells have higher TEER values than the observed values in the human small intestine (Kitaguchi et al., 2021). Other possible differences are expressions and functions of uptake and efflux transporters (Press and Di Grandi, 2008). Further studies are required to confirm these assumptions. Since UGT inhibitors, which cover all types of isoforms, have yet to be reported, the estimation of F_g using UGT inhibitors is limited. Therefore, it is challenging to validate the similarity in the characteristics between Caco-2 cells and hiPSC-SIECs. Hence, additional experimental UGT inhibitor-independent methods, such as UGT knockdown, may be required for validation. Daidzin and genistin, 7-O-glycosides of daidzein and genistein, respectively, are deglycosylated in the small intestine (Murota et al., 2002). Therefore, the differences in the P_{app} values of these compounds may be due to the variation in UGT metabolism and glycosidase activity between Caco-2 cells and hiPSC-SIECs. Further studies must discuss the differences in the P_{app} values of daidzin and genistin because the glycosidase activity of Caco-2 cells and hiPSC-SIECs is not well characterized.

HepaRG cells were used for the prediction of F_h and CL_h because the metabolic activity of these cells is similar to that of cryopreserved human hepatocytes (Zanelli et al., 2012; Bonn et al., 2016). Although cryopreserved human hepatocytes are used as a gold standard to predict CL_h, these cells were not used in this study because they exhibit significant lot-to-lot variation (Araki et al., 2016). Further improvement might be needed to predict CL_h using pooled cryopreserved human hepatocytes, preserving their metabolic activities, e.g., by growing them in 3-dimensional cultures (Lauschke et al., 2019).

V_d was predicted by conducting equilibrium dialysis of human plasma for obtaining experiment- and physicochemical parameter-based f_{ut} values (Berellini and Lombardo, 2019). Compared to the experimental f_{up}, the *in silico*-predicted f_{up} was between 1% and 100%. Values less than 1% were not observed. Highly protein-bound compounds (ochratoxin A, BHT, BHA, and chlorpyrifos) showed significantly higher plasma protein binding rates (> 99.9%) than the *in silico*-derived values. These differences might affect the prediction of V_d values. For example, the *in silico*-derived V_d of BHT was much higher than the *in vitro*-based V_d (5390 L vs. 248 L, respectively).

For predicting CL_r, LLC-PK1 cell-based renal tubular secretion and reabsorption assays were used, as previously reported (Kunze et al., 2014). Daidzein, genistein, and caffeic acid were predicted to be the possible renal secreted compounds ($CL_{r,fil} < CL_{r,org}$), whereas others were identified as reabsorptive compounds ($CL_{r,fil} > CL_{r,org}$). Daidzein and genistein have longer half-lives in patients with end-stage renal disease (Fanti et al., 1999). Although renal excretion of caffeic acid was not reported, it can potentially inhibit human organic anion transporter 1 and 3 (Uwai et al., 2011). The limitation of this method is that the expression and function of some transporters (e.g., organic anion transporters) was insufficient and contributions of renal secretion and reabsorption were relatively smaller than the glomerular filtration ratio. Therefore, further improvement of *in vitro*-based prediction methods might be essential. As LLC-PK1 cells are porcine-derived and might not accurately represent the human RPTEC cell line, human renal proximal epithelium tubular cells-derived cell lines, such as RPTEC-TERT1, SA7K-clone, and ciPTEC, might be better choices for improving predictivity.

Finally, the *in silico*-predicted C_{max} values of 20 food-related compounds were in the range of 0.017-187 times the reported human C_{max} values. By replacing the *in silico*-predicted PBK parameters with *in vitro*-based ones, the prediction accuracy was improved. Then the predicted C_{max} values were almost within 10-fold of those reported in the literature, and half of the compounds were within 3-fold. Previously, Terasaka et al. (2022) reported that most of the predicted C_{max} values of 150 drugs classified as Class 1a and 2 by the extended clearance classification system were within a 6-fold range. Punt et al. (2022) reported that the predicted C_{max} values were within a 5-fold range for 34 of 44 drugs and food-related compounds. Therefore, the authors considered that the prediction accuracy of our *in vitro*-based prediction method was comparable to those previously reported using *in vitro* and *in silico*-based prediction methods.

The *in vitro*-based prediction method employed in our study has two advantages: The first is its focus on predictive methods for food-related compounds with minimal usage of pharmaceutical datasets, which might broaden the applicability domain compared to those of drug-based datasets. The second is its transparency in mimicking each ADME process *in vitro*, which could be more agreeable to safety evaluation assessors emphasizing transparency in the prediction process.

However, the limitation of this method is the limited number of compounds (n = 20) compared with other reports. Further evaluation of compounds might confirm the reliability of our prediction method.

Maximum fold error of the prediction is essential because a large prediction difference might lead to over- or underestimation of the compounds for safety evaluations. Therefore, our *in vitro*-based prediction method was superior to the *in silico*-predicted method because the prediction variability was much lower. Although the C_{max} values of certain food-related compounds evaluated in this study tended to be overestimated, this might not be a problem in evaluating their safety as previously discussed (Punt et al., 2022).

Addition of further ADME-related processes might increase the prediction accuracy of our method. For example, excretion in bile might be an important factor, especially for carboxylic and anionic compounds (Luo et al., 2010). Another possible factor might be the stability of food-related compounds in gastrointestinal fluid. Unlike pharmaceuticals, it is necessary to evaluate the stability of food-related compounds in digestive fluid prior to the absorption process.

Thus, although the consideration of *in vitro*-based parameters is important, improved simulation software for analyzing human plasma concentration is also needed. ACD/Percepta is a simplified compartment-based model that does not include the stability of compounds in the gastrointestinal tract and does not consider the different elimination processes, such as metabolism in the liver, renal elimination, and biliary excretion separately. Without modifying the PK Explorer module, its use can limit the prediction accuracy. The authors experienced this limitation while investigating catechins in the *in vitro* assays, where catechins were difficult to evaluate because of their instability at physiological pH (data not shown).

Out of all the test compounds, only ochratoxin A had underpredicted C_{max} values (0.092-fold). This compound was reported to have extremely low f_{up} values (6×10^{-5}), and its detection sensitivity was close to the detection limit of UPLC-MS/MS. This experimental variability may lead to a difference in predicted V_d (11.7 L) compared to reported V_d (6.9 L), which might lead to lower prediction of C_{max} value. Punt et al. (2022) reported that predicted C_{max} values of ochratoxin A were lower than the observed values; thus, the underestimation of ochratoxin A was not unique in our prediction method. Further research and refinement is needed to resolve this issue.

In conclusion, compared with *in silico*-derived predictions, the authors obtained more accurate and transparent predictions for the C_{max} values of food-related compounds by appropriately combining ADME-related *in vitro* tests and simulation of plasma concentrations. This method can enable accurate safety evaluation of food-related compounds without the need for animal experiments.

References

Araki, T., Iwazaki, N., Ishiguro, N. et al. (2016). Requirements for human iPS cell-derived hepatocytes as an alternative to primary human hepatocytes for assessing absorption, distribution, metabolism, excretion and toxicity of pharmaceuticals. *Fundam Toxicol Sci 3*, 89-99. doi:10.2131/fts.3.89

Baltazar, M. T., Cable, S., Carmichael, P. L. et al. (2020). A next-generation risk assessment case study for coumarin in cosmetic products. *Toxicol Sci 176*, 236-252. doi:10.1093/toxsci/kfaa048

Berellini, G. and Lombardo, F. (2019). An accurate in vitro prediction of human VDss based on the Øie-Tozer equation and primary physicochemical descriptors. 3. Analysis and assess-

ment of predictivity on a large dataset. *Drug Metab Dispos 47*, 1380-1387. doi:10.1124/dmd.119.088914

Bonn, B., Svanberg, P., Janefeldt, A. et al. (2016). Determination of human hepatocyte intrinsic clearance for slowly metabolized compounds: Comparison of a primary hepatocyte/stromal cell co-culture with plated primary hepatocytes and HepaRG. *Drug Metab Dispos 44*, 527-533. doi:10.1124/dmd.115.067769

Bury, D., Alexander-White, C., Clewell, H. J. 3rd et al. (2021). New framework for a non-animal approach adequately assures the safety of cosmetic ingredients – A case study on caffeine. *Regul Toxicol Pharmacol 123*, 104931. doi 10.1016/j.yrtph.2021.104931

Dent, M., Amaral, R. T., Da Silva, P. A. et al. (2018). Principles underpinning the use of new methodologies in the risk assessment of cosmetic ingredients. *Comput Toxicol 7*, 20-26. doi:10.1016/j.comtox.2018.06.001

EFSA – European Food Safety Authority (2014). Modern methodologies and tools for human hazard assessment of chemicals. *EFSA J 12*, 3638. doi:10.2903/j.efsa.2014.3638

Fanti, P., Sawaya, B. P., Custer, L. J. et al. (1999). Serum levels and metabolic clearance of the isoflavones genistein and daidzein in hemodialysis patients. *J Am Soc Nephrol 10*, 864-871. doi:10.1681/ASN.V104864

Gocht, T., Berggren, E., Ahr, H. J. et al. (2015). The SEURAT-1 approach towards animal free human safety assessment. *ALTEX 32*, 9-24. doi:10.14573/altex.1408041

Hallifax, D., Foster, J. A. and Houston, J. B. (2010). Prediction of human metabolic clearance from in vitro systems: Retrospective analysis and prospective view. *Pharm Res 27*, 2150-2161. doi:10.1007/s11095-010-0218-3

Kabeya, T., Mima, S., Imakura, Y. et al. (2020). Pharmacokinetic functions of human induced pluripotent stem cell-derived small intestinal epithelial cells. *Drug Metab Pharmacokinet 35*, 374-382. doi:10.1016/j.dmpk.2020.04.334

Kamiya, Y., Handa, K., Miura, T. et al. (2022). Machine learning prediction of the three main input parameters of a simplified physiologically based pharmacokinetic model subsequently used to generate time-dependent plasma concentration data in humans after oral doses of 212 disparate chemicals. *Biol Pharm Bull 45*, 124-128. doi:10.1248/bpb.b21-00769

Kikuchi, T., Shigemura, S., Ito, Y. et al. (2022). Determination of human FaFg of polyphenols using allometric scaling. *J Toxicol Sci 47*, 409-420. doi:10.2131/jts.47.409

Kilford, P. J., Gertz, M., Houston, J. B. et al. (2008). Hepatocellular binding of drugs: Correction for unbound fraction in hepatocyte incubations using microsomal binding or drug lipophilicity data. *Drug Metab Dispos 36*, 1194-1197. doi:10.1124/dmd.108.020834

Kitaguchi, T., Mizota, T., Ito, M. et al. (2021). Simultaneous evaluation of membrane permeability and UDP-glucuronosyltransferase-mediated metabolism of food-derived compounds using human induced pluripotent stem cell-derived small intestinal epithelial cells. *Drug Metab Dispos 50*, 17-23. doi:10.1124/dmd.121.000605

Kojima, H. (2019). Use of non-animal test methods in the safety assessment of chemicals. *Translat Regulat Sci 1*, 66-72. doi:10.33611/trs.1_66

Kunze, A., Huwyler, J., Poller, B. et al. (2014). In vitro-in vivo extrapolation method to predict human renal clearance of drugs. *J Pharm Sci 103*, 994-1001. doi:10.1002/jps.23851

Lanevskij, K., Didziapetris, R., and Japertas, P. (2010). Trainable QSAR model of plasma protein binding and its application for predicting volume of distribution. *American Chemical Society 240th National Meeting*, MEDI-402. https://bit.ly/3QGaDcp

Lauschke, V. M., Shafagh, R. Z., Hendriks, D. F. G. et al. (2019). 3D primary hepatocyte culture systems for analyses of liver diseases, drug metabolism, and toxicity: Emerging culture paradigms and applications. *Biotechnol J 14*, e1800347. doi:10.1002/biot.201800347

Lea, T. (2015). Caco-2 cell line. In K. Verhoeckx, P. Cotter, I. López-Expósito et al., *The Impact of Food Bioactives on Health*. Berlin, Germany: Springer.

Lu, R., Zhou, Y., Ma, J. et al. (2022). Strategies and mechanism in reversing intestinal drug efflux in oral drug delivery. *Pharmaceutics 14*, 1131. doi:10.3390/pharmaceutics14061131

Luo, G., Johnson, S., Hsueh, M. M. et al. (2010). In silico prediction of biliary excretion of drugs in rats based on physicochemical properties. *Drug Metab Dispos 38*, 422-430. doi:10.1124/dmd.108.026260

Michiba, K., Maeda, K., Shimomura, O. et al. (2022). Usefulness of human jejunal spheroid-derived differentiated intestinal epithelial cells for the prediction of intestinal drug absorption in humans. *Drug Metab Dispos 50*, 204-213. doi:10.1124/dmd.121.000796

Murota, K., Shimizu, S., Miyamoto, S. et al. (2002). Unique uptake and transport of isoflavone aglycones by human intestinal caco-2 cells: Comparison of isoflavonoids and flavonoids. *J Nutr 132*, 1956-1961. doi:10.1093/jn/132.7.1956

Nakamori, F., Naritomi, Y., Hosoya, K. et al. (2012). Quantitative prediction of human intestinal glucuronidation effects on intestinal availability of UDP-glucuronosyltransferase substrates using in vitro data. *Drug Metab Dispos 40*, 1771-1777. doi:10.1124/dmd.112.045476

Nishimuta, H., Sato, K., Yabuki, M. et al. (2011). Prediction of the intestinal first-pass metabolism of CYP3A and UGT substrates in humans from in vitro data. *Drug Metab Pharmacokinet 26*, 592-601. doi:10.2133/dmpk.DMPK-11-RG-034

Ohta, S., Kimura, S., Maejima, D. et al. (2022). Report on 2021 international workshop for non-animal approaches in the food sector (Japan): Current status and avenues for further research. *ALTEX 40*, 350-356. doi:10.14573/altex.2209262

Øie, S. and Tozer, T. N. (1979). Effect of altered plasma protein binding on apparent volume of distribution. *J Pharm Sci 68*, 1203-1205. doi:10.1002/jps.2600680948

Press, B. and Di Grandi, D. (2008). Permeability for intestinal absorption: Caco-2 assay and related issues. *Curr Drug Metab 9*, 893-900. doi:10.2174/138920008786485119

Punt, A., Louisse, J., Beekmann, K. et al. (2022). Predictive performance of next generation human physiologically based ki-

netic (PBK) models based on in vitro and in silico input data. *ALTEX 39*, 221-234. doi:10.14573/altex.210830

Reynolds, D. P., Lanevskij, K., Japertas, P. et al. (2009). Ionization-specific analysis of human intestinal absorption. *J Pharm Sci 98*, 4039-4054. doi:10.1002/jps.21730

Sazonovas, A., Japertas, P., and Didziapetris, R. (2010). Estimation of reliability of predictions and model applicability domain evaluation in the analysis of acute toxicity (LD50). *SAR QSAR Environ Res 21*, 127-148. doi:10.1080/10629360903568671

Sugano, K. (ed.) (2012). *Biopharmaceutics Modeling and Simulations: Theory, Practice, Methods, and Applications*. John Wiley & Sons, Inc. doi:10.1002/9781118354339

Terasaka, S., Hayashi, A., Nukada, Y. et al. (2022). Investigating the uncertainty of prediction accuracy for the application of physiologically based pharmacokinetic models to animal-free risk assessment of cosmetic ingredients. *Regul Toxicol Pharmacol 135*, 105262. doi:10.1016/j.yrtph.2022.105262

Uwai, Y., Ozeki, Y., Isaka, T. et al. (2011). Inhibitory effect of caffeic acid on human organic anion transporters hOAT1 and hOAT3: A novel candidate for food-drug interaction. *Drug Metab Pharmacokinet 26*, 486-493. doi:10.2133/dmpk.dmpk-11-rg-020

Vandecasteele, H. A., Gautier, F., Tourneix, F. et al. (2021). Next generation risk assessment for skin sensitisation: A case study with propyl paraben. *Regul Toxicol Pharmacol 123*, 104936. doi:10.1016/j.yrtph.2021.104936

Waters, N. J. and Lombardo, F. (2010). Use of the Øie-Tozer model in understanding mechanisms and determinants of drug distribution. *Drug Metab Dispos 38*, 1159-1165. doi:10.1124/dmd.110.032458

Yu, L. X., and Amidon, G. L. (1999). A compartmental absorption and transit model for estimating oral drug absorption. *Int J Pharm* 186, 119-125. doi:10.1016/s0378-5173(99)00147-7

Zanelli, U., Caradonna, N. P., Hallifax, D. et al. (2012). Comparison of cryopreserved HepaRG cells with cryopreserved human hepatocytes for prediction of clearance for 26 drugs. *Drug Metab Dispos 40*, 104-110. doi:10.1124/dmd.111.042309

Conflict of interest

The authors have no conflicts of interest.

Data availability

The research data described in the manuscript is available within the article and its supplementary data.